DISTRIBUTION OF AREAL STRAIN ON MERCURY: INSIGHTS INTO THE INTERACTION OF VOLCANISM AND GLOBAL CONTRACTION. G. A. Peterson[1], C. L. Johnson[1,2], P. K. Byrne[3], and R. J. Phillips[4], [1]Departmentof Earth, Ocean and Atmospheric Sciences, University of British Columbia, Vancouver, BC, V6T1Z4 (gpeterso@ubc.eosc.ca), Canada, [2]Planetary Science Institute, Tucson, AZ 85719, USA, [3]Planetary Research Group, Department of Marine, Earth, and Atmospheric Sciences, North Carolina State University, Raleigh, NC 27695, USA, [4]Dept. of Earth and Planetary Sciences and McDonnell Center for the Space Sciences, Washington University, St. Louis, USA.

Introduction: The cooling of Mercury's interior is thought to have decreased the planet's radius by 5–10 km [1,6]. Radial contraction alone predicts an isotropic compressional stress field within Mercury's lithosphere. Indeed, observations from Mariner 10 and MESSENGER show that the surface of Mercury is dominated by shortening structures. However, these features vary in relief, length, and areal density across the lithosphere. Understanding the origin of such regional differences can provide insights into geographical variations in mechanical strength and the timing of global contraction.

The intercrater plains units (hereafter, "ICP") are the oldest (> ~3.8 Ga) and most extensive geological terrain on Mercury, with no evidence of resurfacing since ~4.1 Gy ago. Tectonic structures in the ICP are thought to reflect substantial crustal shortening [1,4,7]. In contrast, the planet's smooth plains units ("SP") show evidence for less ancient (~3.8–3.1 Gy) flood volcanism, with lavas forming deposits ~1-3 km thick [1]. The Northern Smooth Plains ("NSP") is the largest SP deposit on Mercury and is located around the north pole. It is unclear whether shortening structures observed in the SP have accommodated strain from global contraction or if they result from flexure of the lithosphere due to volcanic loading, with only minor contributions from global contraction [1,4,7].

Uncertainty regarding the origin of faulting in the SP arises for several reasons. SP structures have less relief (~400 m) and are generally shorter (~50 km) compared with shortening structures in the ICP, (maximum relief of 1–3 km and lengths of 100–500 km [1]). Further, faulting in the SP may have been influenced by mechanical detachments within volcanic strata that would produce "thin-skinned" faulting, whereas ICP structures may be "thick-skinned" and penetrate as deeply as the brittle–ductile transition depth [1,4,7]. Often, SP structures are referred to as wrinkle ridges, whereas ICP structures are commonly called lobate scarps or high-relief ridges [1], but all feature some combination of folding and thrust faulting. Collectively, these observations and inferences suggest that the total shortening strain, and in particular that due to global contraction, accommodated by the SP is substantially less than that in the ICP [1,4,7,8].

However, recent mapping with MESSENGER data has shown that the SP host more faults per unit area compared with the ICP. The SP comprise ~27% of the total planetary surface, yet hosts ~63% of the mapped shortening structures and 50% of the total mapped fault length [1]. The origin of this difference in fault areal densities is unknown.

Here, we build on this work and analyze the strain concentrations recorded by shortening structures in the ICP and SP. Relative strain amounts can provide insight into the deformational history of the SP, and this has implications for the timing of global contraction and the formation processes responsible for shortening tectonics in these plains.

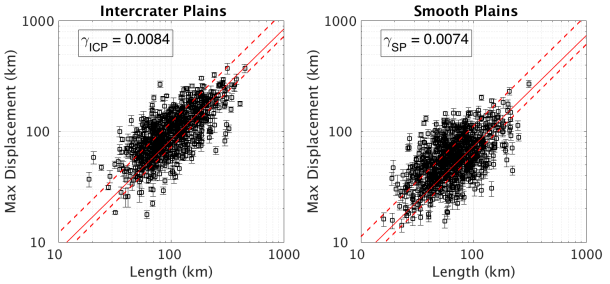

Fig. 1: Length vs. displacement for ICP and SP structures for fault dip angle, θ, of 30°, with the best-fit linear regression (solid red line) and uncertainties (red dashed lines) (see text).

Areal Strain Study: To calculate spatial distributions of areal strain across the lithosphere, global image and topographic data provided by MESSENGER were used to systematically asses the surface morphology of 25% of Mercury's total mapped fault population [1]. We examined 710 structures in the ICP and 786 in the SP, representing 40% and 21% of the individual fault populations, respectively. Structures in Caloris basin, the largest preserved impact feature on Mercury, were ignored as local basin-related deformation may have occurred there [1,7].

For each structure, 10 topographic profiles were extracted perpendicular to fault strike and detrended. For each profile, the background "baseline" elevation away from the fault was determined, and the mean and standard deviation calculated from the profiles. The maximum elevation along-strike was also measured, and the baseline elevation subtracted to find the maximum relief. The baseline standard deviation was taken as the maximum relief error (black error bars in Fig.1).

Strain calculations followed previous studies [1, 2]. The strain, ε, hosted by a population of N faults can be calculated with:

$$\varepsilon = \frac{1}{A}\sum_{k=1}^{N} D_k \cos(\theta) L_k, \quad (1)$$

where L is the fault length and A is the survey area of interest [2]. The maximum displacement (D) of the fault is related to the measured maximum relief (t) and the fault dip (θ) by $D = t/\sin\theta$. In the manner of previous studies [1, 7], we varied θ from 25° to 35°.

In cases where the fault relief was not determined, D was estimated using a D–L scaling factor, γ, determined from the faults with precise relief and length estimates. The red dashed lines in Fig. 1 show the median absolute deviation for the SP and ICP D/L populations, which was used to calculate uncertainties in our regression and hence in the strain estimates.

Estimates in γ for the SP and ICP are given in Table 1 for θ values of 25°, 30°, and 35°. The strain values in Table 1 for the ICP, SP (including specifically the northern smooth plains units, NSP) and the global estimate using all the structures, were determined by summing the strain from displacement–length scaling and the strain from faults with relief estimates.

Fault dip angle	25°	30°	35°
γ_{SP}	0.0087	0.0074	0.0064
γ_{ICP}	0.0010	0.0084	0.0074
Compressional Strain			
SP	0.0070 (-0.0008,+0.0023)	0.0056 (-0.0006,+0.0019)	0.0046 (-0.0005,+0.0015)
NSP	0.0065 (-0.0007,+0.0020)	0.0053 (-0.0006,+0.0016)	0.0043 (-0.0005,+0.0013)
ICP	0.0042 (-0.0003,+0.0009)	0.0034 (-0.0003,+0.0007)	0.0028 (-0.0002,+0.0006)
Global	0.0049 (-0.0009,+0.0025)	0.0039 (-0.0007,+0.0020)	0.0032 (-0.0006,+0.0017)

Table 1: Derived γ for the SP and ICP for θ of 25°, 30°, and 35°. For a given fault dip angle, strain for the SP, NSP, ICP, and the global strain value were calculated using (1).

Shortening Strain: Our results suggest that the SP has accommodated more shortening strain than the ICP, suggesting that the SP has undergone more deformation than previously thought [1,4,7,8]. Fig. 2 shows the cumulative distribution function for strain and for fault counts as a function of L for the SP and ICP. In the SP, 60% of the strain is stored by faults with lengths between 50 and 150 km. This represents 40% of all the faults. However, in the ICP, strain is highly localized by the largest faults: 50% of the strain is stored by the 15% of this fault population with lengths greater than 150 km. Further, although a majority of faults in both units are shorter than 50 km, these faults do not accommodate substantial strain.

Discussion: We suggest that the contrast in morphology and density of compressional tectonics in the SP versus ICP may primarily reflect differences in rheology and the structural character of the lithosphere, rather than the amount of strain accommodated. Under a horizontally uniform stress field induced by global contraction, the greater number of faults in the SP could explain the discrepancy in relief and length between the two units. If the lithosphere in the SP is mechanically weaker, perhaps because of layers of mechanical weakness (décollements) within the lava deposits [1], this could promote the formation of many small landforms such that shortening strain is more evenly distributed in space. Additionally, the higher strain concentration in the SP could result from a combination of subsidence and global contraction acting together. In contrast, shortening strains might concentrate into fewer, larger structures in a more homogenous rock mass, such as the ICP units (which would no longer include such discrete mechanical stratigraphy because of sustained impact bombardment and intrusive activity) [1].

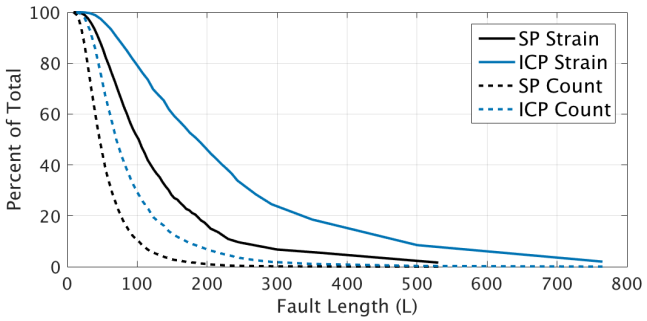

Fig. 2: Cumulative distribution function for fault strain (solid line) and number of faults (dashed line) >= L. Values for the ICP and SP are in blue and black, respectively.

Additionally, the ICP has large spatial variations in crustal thickness, which can vary between 60 and 10 km). This areal variation could localize shortening strains at areas where thick and thin crust are proximal [e.g., 1], such that faults there could accumulate a considerable amount of relief and length. However, the SP has very uniform crustal thickness of ~25 km, which would further have facilitated the more areally homogenous distribution of strain. Finally, results from dislocation modelling suggest that thrust faults in the SP could penetrate to depths of 25 km —inconsistent with the "wrinkle ridge" structures there being thin-skinned in nature [5].

References: [1] Byrne et al. (2014) *Nature Geosci*., 7, 301-307 [2] Cowie et al., (1993) *Geophys. Res. Lett*., 98, 17911- 17920 [3] Head et al., (2012) *Science*, 333, 1853-1856 [4] Melosh, H. J. & McKinnon, W. B. (1988) *Univ. Arizona Press*., 374–400 [5] Peterson et al., (2017) LPS XLVIII Abstract # 2315 [6] Tosi et al. (2015) *Geophys. Res. Lett*., 42, 7327-7335 [7] Watters and Nimmo (2010)., *Cambridge Univ. Press* [8] Watters et al. (2015) *Geophys. Res. Lett*., 42, 3755–3763.